Available online at www.sciencedirect.com
SCIENCE DIRECT®
International Journal of Mass Spectrometry 232 (2004) 195–203
International Journal of Mass Spectrometry
www.elsevier.com/locate/ijms

Branching ratios for the dissociative recombination of hydrocarbon ions II. The cases of $C_4H_n^+$ ($n = 1$–9)

G. Angelova [a], O. Novotny [a,b], J.B.A. Mitchell [a,*], C. Rebrion-Rowe [a], J.L. Le Garrec [a], H. Bluhme [c], K. Seiersen [c], L.H. Andersen [c]

[a] *P.A.L.M.S., U.M.R. No. 6627 du C.N.R.S., Université de Rennes I, 35042 Rennes, France*
[b] *Department of Electronics and Vacuum Physics, Faculty of Mathematics and Physics, Charles University, V. Holesovickach 2, Prague 8, Czech Republic*
[c] *Department of Physics and Astronomy, University of Aarhus, DK-8000 Aarhus C, Denmark*

Received 27 October 2003; accepted 18 December 2003

Abstract

The branching ratios for the dissociative recombination of hydrocarbon ions with general formula $C_4H_m^+$ have been measured using the storage ring technique. It is found that the isomeric state can in some cases give an indication of the preferred dissociation pathways but there are exceptions to this, namely C_4H^+ and $C_4H_5^+$.

Keywords: Dissociative recombination; Isomers; Branching ratios

1. Introduction

Hydrocarbon ions and radicals are found in flames [1,2], industrial material processing devices [3], thermonuclear reactor divertors [4] and the ionospheres of Titan and Jupiter [5,6]. They are also observed in the interstellar environment in interstellar clouds and cometary atmospheres [7]. When starting from simple hydrocarbon precursors, complex ions are produced in a sequence of ion–molecule reactions [8], and are neutralized in the process of dissociative recombination (DR) in which the polyatomic ion collides with an electron and subsequently dissociate into neutral fragments:

$$ABC^+ + e^- \rightarrow \begin{cases} AB + C \\ A + BC \\ AC + B \\ A + B + C \end{cases}$$

Since the resulting neutral molecules and radicals can have a significant influence on the chemistry of the medium, it is important to have information concerning the dominant final channels of the reaction.

In a recent experiment [9], we have used the storage ring technique to determine the branching ratios for the dissociative recombination of $C_4H_9^+$ and $C_4H_5^+$ ions with low energy electrons. It was found that while $C_4H_9^+$ dissociated either to form C_4 or $C_3 + C$ products, i.e.

$$C_4H_9^+ + e^- \rightarrow C_4H_p + H_q$$
$$\rightarrow C_3H_p + CH_q \text{ where } (p+q) = 9$$

$C_4H_5^+$ ions behaved quite differently dissociating primarily to C_4 or to $C_2 + C_2$, i.e.

$$C_4H_5^+ + e^- \rightarrow C_4H_p + H_q$$
$$\rightarrow C_2H_p + C_2H_q \text{ where } (p+q) = 5$$

In a second series of experiments, we have examined the branching ratios for $C_4H_n^+$ ions with "*n*" ranging from 1 to 9 and the results are presented in this paper.

2. Experimental method

The experiment was performed using the electron–ion merged beams technique at the heavy-ion storage ring ASTRID at the University of Aarhus, Denmark. The ions under study were produced from *n*-butane in a Nielsen

* Corresponding author. Tel.: +33-2-23-23-61-92; fax: +33-2-23-23-67-86.
E-mail address: mitchell@univ-rennes1.fr (J.B.A. Mitchell).

1387-3806/$ – see front matter © 2004 Elsevier B.V. All rights reserved.
doi:10.1016/j.ijms.2003.12.013

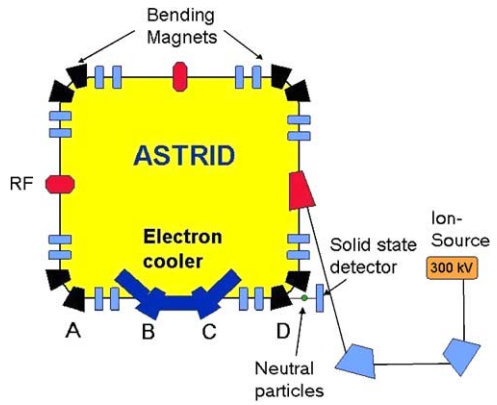

Fig. 1. Layout of ASTRID storage ring showing beam injection, electron cooler and neutral particles detection system. Magnets are labeled A–D.

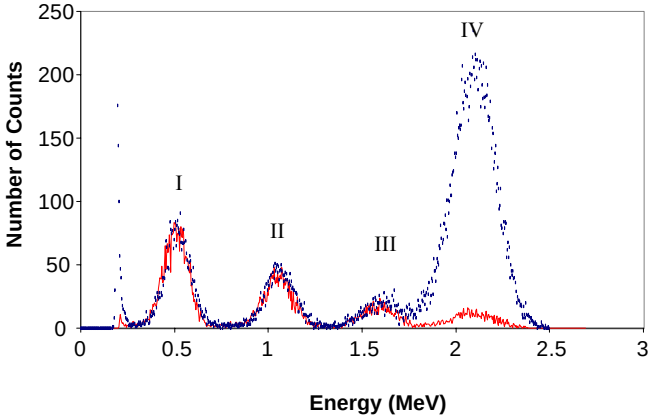

Fig. 2. Pulse height spectrum for neutral products arising from C_4H^+ ions due to electron–ion and background gas collisions (electron-beam on, dotted curve). With the electron beam off (continuous curve), only the latter are present. The abscissa is calibrated in terms of the energies of the arriving particles. The high peak on the left is part of the electron noise of the detector, truncated by using a pulse discriminator.

electron impact source, accelerated to 150 keV and injected into the storage ring (shown in Fig. 1).

In ASTRID, the ions are accelerated to 2.5 MeV and this process takes about 4 s to accomplish. An electron beam of known energy, formed in the electron cooler assembly is merged with and de-merged from the ions in the storage ring using the dipole magnets B and C shown in Fig. 1. The field of these magnets is rather weak and has little effect on the fast heavy ion beam. The electron beam, can be turned on and off by removing the bias from a grid in front of the cathode. The electron velocity is tuned to be essentially identical to that of the ions so that a very low centre-of-mass collision energy can be achieved.

Neutrals, formed in the straight section between magnets A and D (Fig. 1) pass un-deflected through magnet D and are detected by a surface-barrier detector located at a distance of 6 m from the exit of the electron cooler magnet C. There are two sources for these neutrals. One involves interaction of the stored ion beam with the background gas in the storage ring which is maintained at a pressure of about 10^{-11} Torr. The other source is interaction of the ions with the electron beam. For low centre-of-mass collision energies, this interaction is only due to dissociative recombination. When molecular ions undergo dissociation in a storage ring, the resulting fragments carry away with them kinetic energies that are distributed according to the fragment mass since they continue their passage through the machine with essentially the same velocity as the primary ion. (Velocity changes due to the release of dissociation energy are small compared with the primary ion velocity and for the purposes of the present discussion can be neglected.) The surface barrier detector is energy sensitive and so is capable of distinguishing between fragments that arrive individually with differing masses.

Fig. 2 shows the pulse height spectra for products arising from C_4H^+ ions, accumulated with the electrons on and off. The four peaks correspond to molecular fragments with 1, 2, 3 or 4 carbon atoms. In fact these peaks are made up of sub-peaks due to fragments with differing numbers of hydrogen atoms but the resolution is insufficient to distinguish between them. There should also be peaks due to released hydrogen atoms and molecules but these lie low in energy and fall into the electronic noise of the detector that is removed using a discriminator. We are thus unable to determine by direct means, the number of hydrogen atoms that are distributed between the fragments. We can, however, observe the scission of C–C bonds.

In the absence of the electron beam, the peaks (I–IV) in the neutral particle spectrum arise from background gas reactions such as

$$C_4^+ + X \rightarrow C_4 + X^+ \quad (1a)$$

$$C_4^+ + X \rightarrow C_3 + C^+ + X \quad (1b)$$

$$C_4^+ + X \rightarrow C_2 + C_2^+ + X \quad (1c)$$

$$C_4^+ + X \rightarrow C + C_3^+ + X \quad (1d)$$

where X is a background gas molecule and we have ignored the hydrogen atoms. The ionic species are deflected away by the dipole magnet D and so do not reach the detector.

When the electron beam is on, in addition to these background reactions, the following recombination processes occur:

$$e^- + C_4^+ \rightarrow C_4 \quad (2a)$$

$$e^- + C_4^+ \rightarrow C_3 + C \quad (2b)$$

$$e^- + C_4^+ \rightarrow C_2 + C_2 \quad (2c)$$

$$e^- + C_4^+ \rightarrow C_2 + C + C \quad (2d)$$

Since the recombination fragments are all neutral, they arrive simultaneously at the detector, appear as if they were a single full-energy particle and accumulate in peak IV.

In order to distinguish between ion-background gas processes and ion–electron processes, the electron beam is

chopped electrostatically and measurements of the neutrals are performed when the electrons are on and when they are off. Neutrals due to recombination are thus determined by subtracting the two measured count rates.

2.1. Branching ratio measurement

The goal of the present experiment is to determine the branching ratios, i.e., the relative proportions of the four possible recombination channels (2a)–(2d) that give rise to products having different combinations of carbon atoms. By limiting the probability of all the particles reaching the detector by placing a mesh grid with a known transmission T in front its entrance window [10], one is able to distinguish between the various recombination channels since the probability of one atom or molecule reaching the detector is T, for two atoms or molecules it is T^2, etc. and $T < 1$. When not all particles from a given recombination event arrive at the detector, those that do will therefore, fall into lower energy channels since not all the energy is deposited. We can analyze the contributions from each of the recombination channels that fall into peaks I–IV but one must take into account not only the probability of a particle passing through the grid and being detected but the probability for a particle to be stopped by the grid and thus fail to be detected, and the number of ways that a given situation can occur. Thus, the number particles in peaks I–IV being N_{I}, N_{II}, N_{III} and N_{IV} is given by

$$N_{\mathrm{I}} = T(1-T)N_{2\mathrm{b}} + 2T(1-T)N_{2\mathrm{d}}$$

$$N_{\mathrm{II}} = 2T(1-T)N_{2\mathrm{c}} + \{2T(1-T) + T^2(1-T)\}N_{2\mathrm{d}}$$

$$N_{\mathrm{III}} = T(1-T)N_{2\mathrm{b}} + 2T^2(1-T)N_{2\mathrm{d}}$$

$$N_{\mathrm{IV}} = TN_{2\mathrm{a}} + T^2N_{2\mathrm{b}} + T^2N_{2\mathrm{c}} + T^3N_{2\mathrm{d}}$$

where $N_{2\mathrm{a}}$, $N_{2\mathrm{b}}$, $N_{2\mathrm{c}}$ and $N_{2\mathrm{d}}$ are the fractions of the total number of recombinations that yield channels 2a, 2b, 2c and 2d, respectively. This method has been used previously in a large number of branching ratio measurements with hydrocarbon molecular ions at ASTRID [9,11] and also at CRYRING at the Manne Siegbahn Laboratory in Sweden [12–17].

A series of equations was presented in [9] that allowed for corrections due to light fragments missing the detector. For all the measurements described here, it was verified that in fact there were no such losses. This was done by examining the measured counts without a grid in front of the detector and verifying that the only difference between the (electrons-on) and (electrons-off) count rates, occurred in the fourth peak (such is the case for the spectra shown in Fig. 2).

The actual measurement was performed using two separate grids with measured [18] transmission values $T_1 = 0.675$ and $T_2 = 0.235$ known to an accuracy of ±0.5%. The values of $N_{\mathrm{I–IV}}$, used as input into the probability equations were determined from the difference in measured pulse height spectra (electrons on minus electrons off) by fitting the resulting individual peaks (see for example, Fig. 3) using a Levenberg–Marquart non-linear fitting method [19] assuming that they are formed from a set of Gaussian peaks. (A given peak, arising from the recombination of an ion $C_4H_n^+$ will consist of contributions from C_mH_p fragments where m is the peak number and $P \leq n$.) The pulse height analyzer has an associated live-time that is a function of the input count rate, and since this is different during the electrons-on and electrons-off cycles, a correction must be made for this by multiplying the electrons-on count rate by the ratio of the (electrons-off)/(electrons on) live-times. A typical value for this factor is 0.95. It is also possible that a high peak can be contaminated by pulses destined for a low peak due to two such pulses arriving at the same time. This effect is known as pulse pile-up and care was taken to avoid this.

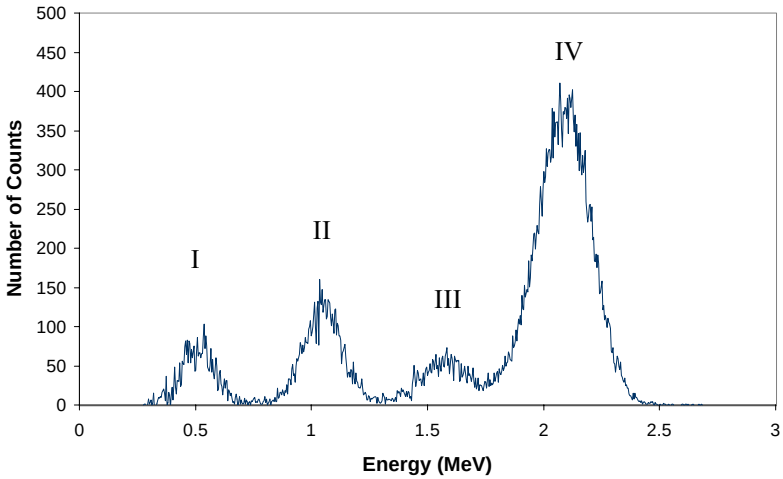

Fig. 3. Pulse height spectrum of neutral recombination products arising from electron collisions with C_4H^+. The re-distribution of the neutral products into lower energy peaks was achieved by placing a grid with transmission $T = 0.675$ in front of the detector (see text). The background contribution to the spectrum has been subtracted off and the electronic noise peak removed for clarity.

A χ^2 based error analysis method taking account of statistical counting errors and errors due to the fitting procedures, pulse pile-ups and live-time corrections is applied to the data and the results of this, along with the branching ratio measurements are presented below.

3. Results and discussion

It is important to have some understanding of the structural identity of the ion undergoing recombination in these experiments. In the absence of other information, and due to the long storage time of the ions (4 s) before recombination, we make the assumption that if different isomeric forms of the ion are initially created, they have time to relax to the lowest lying form. The likely isomeric forms will be discussed for each ion individually with the exception of $C_4H_9^+$ and $C_4H_5^+$ that have already been discussed in [9].

The branching fractions measured for the $C_4H_n^+$ ions with "*n*" ranging from 1 to 9 are listed in Table 1 along with the estimated errors, determined using the procedures discussed above are shown. The data shown for $C_4H_5^+$ and $C_4H_9^+$ is slightly different from that originally published in [9] due to the use of the more detailed data analysis method, discussed above.

In no case is the channel involving $C_2 + C + C$ seen to be active. For all isomers, the loss of at least one hydrogen atom or molecule, without scission of the C–C bond is possible and this would yield a C_4 product. If we look globally at this table, we note firstly that C_4H^+ behaves quite differently from the other ions in the series. Secondly, $C_4H_2^+$, $C_4H_3^+$ and $C_4H_4^+$ are rather similar. Thirdly, the $C_2 + C_2$ ratio declines between $C_4H_5^+$ and $C_4H_8^+$ while the $C_3 + C$ ratio increases. Generally, the measurements were performed at zero centre-of-mass energy (where the electron and ion beams have equal velocities) and *n*-butane as the source gas. For, $C_4H_8^+$ however, a measurement was also performed at 0.5 eV centre-of-mass energy but no significant difference was seen in the measured ratios. In addition, $C_4H_9^+$ was prepared using both *n*-butane and *iso*-butane source gases but again no difference was seen.

Table 1
Branching fractions for the dissociative recombination of $C_4H_n^+$ ions

Species	C_4 (%)	$C_3 + C$ (%)	$C_2 + C_2$ (%)
C_4H^+	43.8 ± 1.2	28.2 ± 2.1	27.9 ± 1.7
$C_4H_2^+$	78.4 ± 1.3	4.0 ± 1.6	17.7 ± 1.5
$C_4H_3^+$	76.0 ± 0.5	6.3 ± 0.4	17.8 ± 0.4
$C_4H_4^+$	76.6 ± 2.7	6.3 ± 2.0	17.1 ± 2.1
$C_4H_5^+$	46.0 ± 5.4	9.3 ± 2.1	44.7 ± 5.3
$C_4H_6^+$	58.9 ± 3.5	9.0 ± 1.5	32.1 ± 3.4
$C_4H_7^+$	19.8 ± 4.4	65.5 ± 5.9	14.7 ± 3.4
$C_4H_8^+$	30.5 ± 3.1	63.5 ± 3.2	6.1 ± 2.1
$C_4H_9^+$	57.5 ± 4.1	41.1 ± 3.8	1.5 ± 2.6

Fig. 4. The most stable isomeric forms of C_4H^+.

3.1. C_4H^+

The pulse height spectrum of the recombination products (with the background products subtracted off) obtained with a grid ($T = 0.675$) in front of the detector is presented in Fig. 3. It is seen that signal appears in each of the four peaks indicating that the dissociation channels leading to C_4, $C_3 + C$ and $C_2 + C_2$ are certainly produced.

Very little is known concerning the geometry and the relative stability of the isomers of C_4H^+ and most experimental data on the structure of this ion and its neutral counterpart are essentially spectroscopic [20]. It is however, widely accepted that the most stable structure of the corresponding neutral radical, butadiyne (C_4H) is linear [21–23], with an acetylenic structure, and that one of the stable isomers of C_4H^+ has the same geometry [24]. Calculations by Lammertsma [25] based on the isoelectronic relationship of $C_4H_2^{2+}$ with C_4H^+ have suggested that another low lying structure for C_4H^+ is a bicyclic four member ring (Fig. 4) and that branched and three-membered-ring structures are higher in energy. The energy difference between the linear and the bicyclic isomer is very small (8 meV), and is positive or negative according to the level of theory. We shall consider that both isomers can be present in our beam. From the arguments given in [26], one can estimate that the ionization potential is in excess of 12 eV. (For C_4 it is 12.54 eV [20].) The heat of formation for C_4H is 6.73 eV [27]. From this information and from a knowledge of the heats of formation of possible products (see Appendix A) it is found that channels involving the breaking of a single C–C bond or a C–H bond are open (exothermic) while those involving the scission of two carbon–carbon bonds are closed.

It is not easy to understand the behaviour of this ion by just considering the isomeric structures as dissociation towards $C_3 + C$ would not seem to be favoured, given that for the linear isomer, this would imply the rupture of a triple bond. $C_2 + C_2$ formation from this isomer would seem much more likely yet this is not reflected strongly in the observed branching ratios. Both isomeric forms would be expected to yield a C_4 product and indeed this is the major dissociation channel.

It would seem that a re-structuration of the neutral molecule occurs following electron capture. The bond dissociation energies of linear C_4H in excited states have been calculated [28] and in fact it is found that while the single C–C bond maintains its length and hence its bonding energy as one goes from the ground to higher excited states, the triple bond elongates eventually becoming weaker than the single bond. Calculations of energy thresholds for the photodissociation of the C_4H radical indicate that while

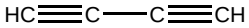

Fig. 5. The most stable isomeric form of neutral C_4H_2.

7.12 eV are necessary for the scission to form $C_2 + C_2H$, only 5.88 eV is needed to form $C_3 + CH$. (Dissociation to $C_4 + H$ requires 5.71 and 6.33 eV to form $C + C_3H$.) Dissociation following electron capture requires the system to descend through one or more excited states and so in this case it is in fact not unreasonable to expect that the $C_3 + C$ channel would be important. Theoretical analysis of the recombination process is clearly needed however, to establish exactly what the dissociation route is.

3.2. $C_4H_2^+$

No study about the isomeric forms of $C_4H_2^+$ is available, and we make the assumption that in our experiment, we have diacetylene radical cations. Diacetylene (Fig. 5) is the most stable neutral isomeric form [29,30], and its vertical ionisation energy is 10.3 eV [20].

The energy release (see Appendix A) allows either one triple or one single C–C bond to be broken, leading to either $C_3 + C$ or $C_2 + C_2$ but the $C_2 + C + C$ channel is closed.

The pulse height spectrum obtained using a grid ($T = 0.675$) is shown in Fig. 6. (Similar spectra are found for $C_4H_3^+$ and $C_4H_4^+$ ions.) It is seen here that signal only appears in peaks II and IV indicating that only the $C_2 + C_2$ and C_4 channels are active. As seen from Table 1, the predominant dissociation pathway is C_4 accounting for 78.4% of all dissociations. 18% of the reaction goes to $C_2 + C_2$ and only 4% (±1.6%) goes to the $C_3 + C$ channel. As expected, the $C_2 + C + C$ channel is negligible.

3.3. $C_4H_3^+$

The lowest energy structure of $C_4H_3^+$ [31] is illustrated in Fig. 7. The most stable neutral form is the α-ethinylvynil radical [32]. The heat of formation of $C_4H_3^+$ is 12.49 eV [33]. The recombination behavior of this ion is similar to that for $C_4H_2^+$. The predominant dissociation pathway is C_4 (76%) with 18% of the reaction going to $C_2 + C_2$. The $C_3 + C$ channel accounts for just 6% of the total.

3.4. $C_4H_4^+$

$C_4H_4^{\bullet+}$ ions are common products of the unimolecular dissociation of unsaturated/cyclic molecules and have therefore been the subject of a large number of experimental investigations (see [34] and [35] and references cited therein). The consensus is that in the gas phase, at least two isomeric populations are formed and co-exist. Their exact nature depends on their precursors, but one form is cyclic and the other linear [36]. The linear structure corresponds to vinylacetylene ($VA^{\bullet+}$) and the cyclic form is usually presumed to be methylenecyclopropene ($MCP^{\bullet+}$) [37]. Ions having one of the other classical structures butatriene ($BT^{\bullet+}$) and cyclobutadiene ($CB^{\bullet+}$) are expected to be formed only by fragmentation of precursors having structures close to BT or CB [38]. The four classical isomers are represented in Fig. 8, and the relative energies of the ionic and neutral forms are listed in Table 2.

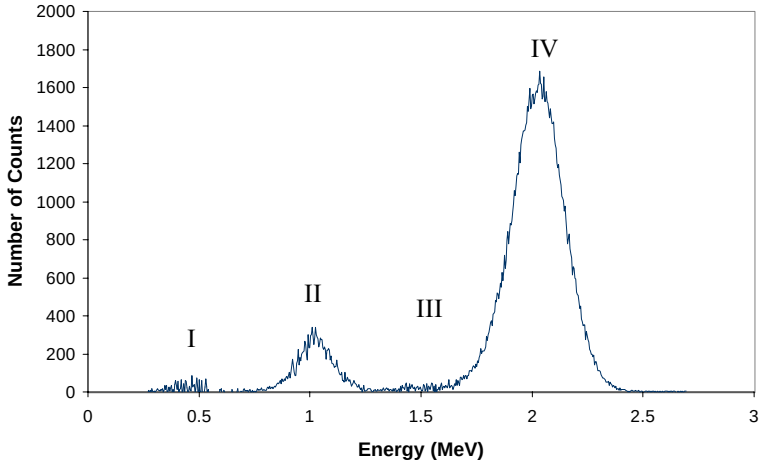

Fig. 6. Pulse height spectrum of neutral recombination products arising from electron collisions with $C_4H_2^+$ with a grid with transmission $T = 0.675$ placed in front of the detector. The background contribution to the spectrum has been subtracted off and the electronic noise peak removed for clarity.

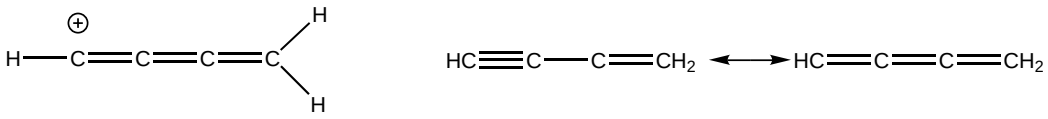

Fig. 7. The most stable $C_4H_3^+$ ion (left) and the α-ethinylvynil radical (right).

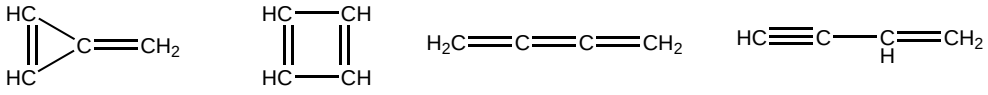

Fig. 8. The four most stable isomers of C_4H_4.

Table 2
Relative energies (eV) of the ionic and neutral forms of C_4H_4

	Neutrals		Ions	
	[37]	[39]	[37]	[38]
MCP	1.07	0.89	0	0
CB	1.46	1.48	0.31	0.39
BT	0.34	0.17	0.32	0.26
VA	0	0	0.43	0.48

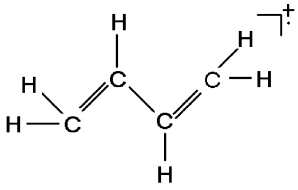

Fig. 9. Structure of *trans*-butadiene.

From this table, it can be stated that if $MCP^{\bullet+}$ is the absolute minimum on the radical cation potential energy surface, VA is the most stable neutral.

The predominant dissociation pathway is C_4 with 17% of the reaction going to $C_2 + C_2$. The $C_3 + C$ channel accounts for 6% of the reaction. This is similar to the cases of $C_4H_2^+$ and $C_4H_3^+$.

3.5. $C_4H_6^+$

Trans-butadiene (Fig. 9) is the most stable form of the ion [40–43] and of the neutral [20]. The predominant dissociation pathway is seen to be $C_2 + C_2$ with C_4 being twice as likely. The $C_3 + C$ accounts for 9% of the dissociations. This is consistent with the isomeric structure shown.

3.6. $C_4H_7^+$

The $C_4H_7^+$ ions and $C_4H_7^\bullet$ radicals (Fig. 10) have been extensively studied from the energetic [44,45], mechanistic [46] and kinetic [47] points of view. This interest is mainly due to the cyclopropylcarbinyl–cyclobutyl–homoallyl system, in which the inter-conversion is so fast that the three

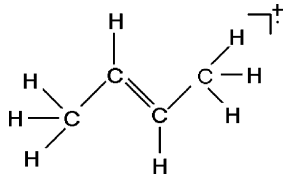

Fig. 11. The *trans*-2-butene isomer of $C_4H_8^+$.

$C_4H_7^+$ structures have been discussed as resonance forms of a non-classical ion [48]. Rapid collision-induced rearrangements of less stable isomers to the lower lying 1-methylallyl cation (1-buten-3-yl cation) have been observed [45]. This cation in its *trans* structure [49] is the global minimum on the $C_4H_7^+$ potential energy surface and is 0.39 eV more stable than the former cited system [50]. Its neutral counterpart is not the most stable radical, and lies 4 meV higher in energy than the 2-methylallyl radical [51]. The energy release in the recombination reaction is large enough to break either one double C–C bond, or two simple C–C bonds and so the $C_2 + C + C$ channel is therefore formerly open. In fact our measurement shows this channel to be negligible.

The $C_3 + C$ channel is dominant, being almost three times more important than the C_4 channel. The $C_2 + C_2$ channel accounts for about 15% of the total.

3.7. $C_4H_8^+$

It is known that when $C_4H_8^+$ ions are formed, they primarily consist of a mixture of several isomers that rearrange to the thermodynamically most stable structure before fragmentation [52–55]. Although some disagreements about the isomerisation mechanisms exist [56,57], the *trans*-2-butene cation (Fig. 11) is unambiguously the most stable ion ([55,58] and references therein). The same situation as for $C_4H_7^+$ prevails, that is, the neutral counterpart of the most stable cation is not the most stable neutral, and the most stable C_4H_8 isomer is isobutene, which lies 70 meV lower than *trans*-2-butene.

The pulse height spectrum for this ion is shown in Fig. 12 and it can be seen that signal appears in peaks I, III and IV indicating that the dissociation pathways leading to $C + C_3$

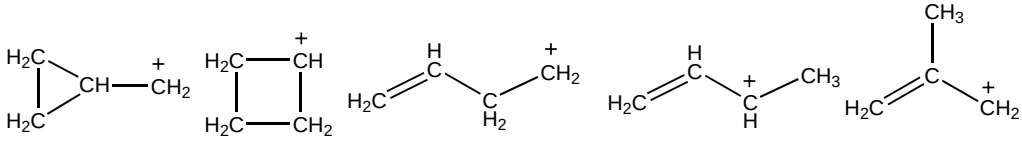

Fig. 10. From left to right: cyclopropylcarbinyl, cyclobutyl, homoallyl, *trans*-1-methylallyl, 2-methylallyl.

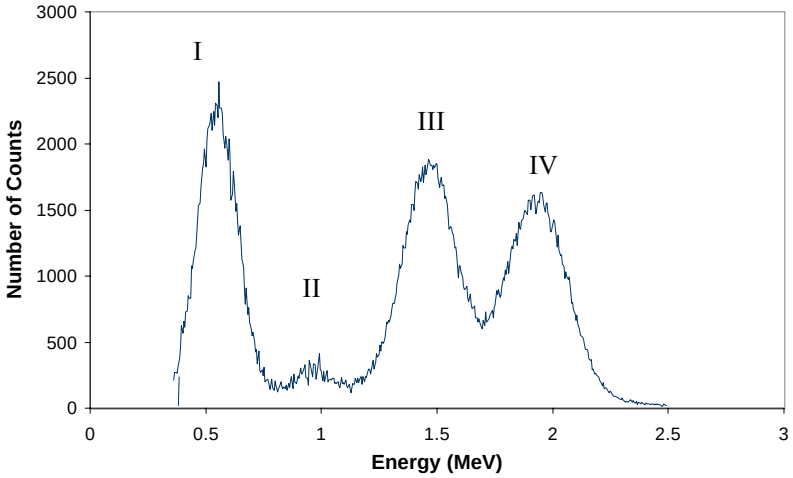

Fig. 12. Pulse height spectrum of neutral recombination products arising from electron collisions with $C_4H_8^+$ with a grid of transmission $T = 0.675$ placed in front of the detector. The background contribution to the spectrum has been subtracted off and the electronic noise peak removed for clarity.

and to C_4 are produced. Though the $C_2 + C + C$ channel is energetically allowed, it is seen to be negligible.

The predominant dissociation pathway is seen to be C_3+C which is twice as likely as a C_4 dissociation. The $C_2 + C_2$ accounts for only 6% of the total. Again this is consistent with the isomeric structure.

4. Conclusion

Upon reviewing the family of ions discussed here, it is clear that while the initial isomeric form of the ion undergoing recombination allows one to make an educated guess as to the likely dissociation pathways, exceptions such as C_4H^+ and $C_4H_5^+$ show that this is not always accurate. Indications are that in general, single bonds tend to be those that are broken though the rupture of a double bond or even a triple bond is not ruled out (e.g., as in C_4H^+). The exact bond strengths in non-classical molecules are often unknown. Typical values for hydrocarbons in their ground states are 3.82 eV for a simple C–C bond in *n*-alkanes [59] (7.2 ± 0.3 eV) for a double bond and (8.8 ± 1.2 eV) for a triple one [60]. Reliable bond dissociation energies values are not available for strained cyclic compounds [61]. More generally, an inverse linear relationship exists between the bond length and its dissociation energy [61]. When dealing with dissociative recombination, the system must pass through one or more excited states of the neutral parent radical following electron capture and the bond lengths may be quite different in these states from those for the ground state radical. Hence, structural calculations that are usually performed for isomers in their ground states do not necessarily apply to the processes discussed here. The reason why this should be so in some cases though not in others must be found in detailed calculations of excited state structures and by a clearer understanding of the mechanism for hydrocarbon ion recombination. In all cases studied here, the channel resulting from the scission of two carbon–carbon bonds was found to be negligible.

Acknowledgements

The authors would first of all like to thank the operators and technical staff at the Institute for Storage Ring Facilities at the University of Aarhus (ISA) for their expertise and for their greatly appreciated assistance. Financial assistance was provided by the *European Community—Access to Infrastructure Action of the Improving Human Potential Programme* and in part by the *European Community's Research Training Networks Programme under contract HPRN-CT-2000-0142, ETR*. This work was supported by the Danish National Research Foundation through the Aarhus Center for Atomic Physics (ACAP).

Appendix A

The kinetic released during the recombination process:

$$A^+ + e^- \rightarrow B + C + KER$$

is given by

$$\begin{aligned} KER\,(eV) &= \Delta H_f^\circ(A^+) - [\Delta H_f^\circ(B) + \Delta H_f^\circ(C)] \\ &= \Delta H_f^\circ(A) + IP(A) - [\Delta H_f^\circ(B) + \Delta H_f^\circ(C)] \end{aligned}$$

where IP is the ionisation potential of the parent neutral radical and ΔH_f° are the standard heats of formation of the respective entities. The values for these quantities used to produce the following tables are taken from refs. [23,30] except where specifically noted (Table A.1).

Table A.1
Values for the heat of formation ΔH_f° (kJ/mol) and the ionisation potential IP (eV) for products of the recombination reactions discussed in this paper

Compound	ΔH_f° (kJ/mol)	IP (eV) {kJ/mol}
H	218	
H_2	0	
C	717	
C_2	831	
C_3	840	
C_4	1034	
CH	597	
CH_2	425	
CH_3	146	
CH_4	−75	
C_2H	569	
C_2H_2	227	
C_2H_3	299	
C_2H_4	53	
C_2H_5	119	
C_2H_6	−84	
C_3H (cyclic)	684	9.06 {874}
C_3H_2 (cyclic)	477	9.15 {883}
C_3H_3 (CH_2CCH)	347	8.67 {837}
C_3H_4 (CH_3CCH)	185	10.37 {1001}
C_3H_5 (CH_2CHCH)	164	8.18 {789}
C_3H_6 (propylene)	20	9.73 {938}
C_3H_7 (*iso*-propyl)	95	7.37 {711}
C_3H_8	−104	11.0 {1061}
C_4H (CHCCC)	648.9	12.54 {1210}
C_4H_2 (CHCCCH)	464	10.17 {981}
C_4H_3 ($CHCCCH_2$)	465.8	7.66 {739.5}
C_4H_4 ($CHCCHCH_2$)	295	9.58 {925}
C_4H_5 (cyclic)	201.2	7.95 {767}
C_4H_6 ($CH_2CHCHCH_2$)	108.8	9.08 {876}
C_4H_7 (*iso*)	83.2	7.90 {762}
C_4H_8 (*iso*)	−17.9	9.19 {887}
C_4H_9 (*iso*)	48	6.70 {647}

References

[1] A.B. Fialkov, Prog. Energy Combust. Sci. 23 (1997) 399.
[2] S. Williams, A.J. Midley, S.T. Arnold, P.M. Bench, A.A. Viggiano, R.A. Morris, L.Q. Maurice, D. Carter, AIAA J. 99 (1999) 4907.
[3] K. Hassouni, X. Duten, A. Rousseau, A. Gicquel, Plasma Sources Sci. Technol. 10 (2001) 61.
[4] D.A. Alman, D.N. Ruzic, J.N. Brooks, Phys. Plasmas 7 (2000) 1421.
[5] C.N. Keller, V.G. Anicich, T.E. Cravens, Planet Space Sci. 46 (1998) 1157.
[6] J.L. Fox, Dissociative recombination: theory, experiment and applications III, in: D. Zajfman, J.B.A. Mitchell, D. Schwalm, B.R. Rowe (Eds.), World Scientific, Singapore, 1996, p. 40.
[7] P. Ehrenfreund, S.B. Charnley, Annu. Rev. Astron. Astrophys. 38 (2000) 427.
[8] Herbst, Annu. Rev. Phys. Chem. 46 (1995) 27.
[9] J.B.A. Mitchell, C. Rebrion-Rowe, J.L. Le Garrec, G. Angelova, H. Bluhme, K. Seiersen, L.H. Andersen, Int. J. Mass Spectrom. 227 (2003) 273.
[10] J.B.A. Mitchell, J.L. Forand, C.T. Ng, D.P. Levac, R.E. Mitchell, P.M. Mul, W. Claeys, A. Sen, J.Wm. McGowan, Phys. Rev. Lett. 51 (1983) 885.
[11] L. Vejby-Christensen, L.H. Andersen, O. Heber, D. Kella, H.B. Pedersen, H.T. Schmidt, D. Zajfman, Astrophys. J. 483 (1997) 531.
[12] J. Semaniak, A. Larson, A. Le Padellec, C. Stromholm, M. Larsson, S. Rosen, P. Peverall, H. Danared, N. Djuric, G.H. Dunn, S. Datz, Astrophys. J. 498 (1998) 886.
[13] A. Larson, A. Le Padellec, J. Semaniak, C. Stromholm, M. Larsson, S. Rosen, R. Peverall, H. Danared, N. Djuric, G.H. Dunn, S. Datz, Astrophys. J. 505 (1998) 459.
[14] A. Derkatch, A. Al-Khalili, L. Vikor, A. Neau, W. Shi, H. Danared, M.af Ugglas, M. Larsson, J. Phys. B 32 (1999) 3391.
[15] A. Derkatch, B. Minaev, M. Larsson, Phys. Scripta 67 (2003) 407.
[16] S. Kalhori, A.A. Viggiano, S.T. Arnold, S. Rosen, J. Semaniak, A.M. Derkatch, M.af Ugglas, M. Larsson, Astron. Astrophys. 391 (2002) 1159.
[17] A. Ehlerding, S.T. Arnold, A.A. Viggiano, S. Kalhori, J. Semaniak, A.M. Derkatch, S. Rosen, M. af Ugglas, M. Larsson, J. Phys. Chem. A 107 (2003) 2179.
[18] M.J. Jensen, Ph.D. Thesis, Aarhus University, 2001.
[19] W.H. Press, S.A. Teukolsky, W.T. Veterrling, B.P. Flannery, Numerical Recipes in Fortran, Cambridge University Press, 1992.
[20] NIST Standard Reference Database Number 69, The National Institute of Standards and Technology (NIST), http://webbook.nist.gov/.
[21] M. Kolbuszewski, Astrophys. J. Part 2 432 (1) (1994) L63.
[22] D.E. Woon, Chem. Phys. Lett. 244 (1995) 45.
[23] S. Wilson, S. Green, Astrophys. J. 240 (1980) 968.
[24] K. Lammertsma, J.A. Pople, P.v.R. Schleyer, J. Am. Chem. Soc. 108 (1986) 7.
[25] K. Lammertsma, J. Am. Chem. Soc. 108 (1986) 5127.
[26] C. Aubrey, J.L. Holmes, Int. J. Mass Spectrom. 200 (2000) 277.
[27] http://web.mit.edu/anish/www/thermpub.doc.
[28] S. Graf, J. Geiss, S. Leutwyler, J. Chem. Phys. 114 (2001) 4542.
[29] C.E. Dykstra, C.A. Parsons, C.L. Oates, J. Am. Chem. Soc. 101 (1979) 1962.
[30] C.L. Collins, C. Meredith, Y. Yamaguchi, H.F. Schaefer III, J. Am. Chem. Soc. 114 (1992) 8694.
[31] S. Petrie, J.S. Knight, C.G. Freeman, R.G.A.R. Maclagan, M.J. McEwan, P. Sudkeaw, Int. J. Mass Spectrom. Ion Process. 105 (1991) 43.
[32] T. Ha, E. Gey, J. Mol. Struct. (Theochem.) 306 (1994) 197.
[33] M. Schwell, F. Dulieu, C. Gée, H.-W. Jochims, J.-L. Chotin, H. Baumgartel, S. Leach, Chem. Phys. 260 (2000) 261.
[34] M. Zhang, B.K. Carpenter, F.W. McLafferty, J. Am. Chem. Soc. 113 (1991) 9499.
[35] G. Koster, W.J. Van der Hart, Int. J. Mass Spectrom. Ion Process. 163 (1997) 81.
[36] S.W. Staley, T.D. Norden, J. Am. Chem. Soc. 111 (1989) 445.
[37] V. Hrouda, M. Roeselova, T. Bally, J. Phys. Chem. A 101 (1997) 3925.
[38] G. Koster, W.J. Van der Hart, Int. J. Mass Spectrom. Ion Process. 163 (1997) 169.
[39] H. Kollmar, F. Carrion, M.J.S. Dewar, R.C. Bingham, J. Am. Chem. Soc. 103 (1981) 5292.
[40] V. Hrouda, P. Carsky, M. Ingr, Z. Chval, G.N. Sastry, T. Bally, J. Phys. Chem. A 102 (1998) 9297.
[41] G.N. Sastry, T. Bally, V. Hrouda, P. Carsky, J. Am. Chem. Soc. 120 (1998) 9323.
[42] W.J. Van der Hart, Int. J. Mass Spectrom. Ion Process. 208 (2001) 119.
[43] C.H. Martin, R.L. Graham, K.F. Freed, J. Phys. Chem. 98 (1994) 3467.
[44] M. Saunders, K.E. Laidig, K.B. Wiberg, P. von Rague Schleyer, J. Am. Chem. Soc. 110 (1988) 7652.
[45] S.G. Lias, P. Ausloos, Int. J. Mass Spectrom. Ion Process. 81 (1987) 165.
[46] R.F.W. Bader, K.E. Laidig, J. Mol. Struct. (Theochem.) 261 (1992) 1.
[47] D.M. Smith, A. Nicolaides, B.T. Golding, L. Radom, J. Am. Chem. Soc. 120 (1998) 10223.
[48] T.H. Morton, Advances in Gas Phase Ion Chemistry, vol. 4, Elsevier, Amsterdam, 2001, p. 213.
[49] J.C. Traeger, J. Phys. Chem. 90 (1986) 4114.
[50] W. Koch, B. Liu, D.G. DeFrees, J. Am. Chem. Soc. 110 (1988) 7325.

[51] J.C. Schultz, F.A. Houle, J.L. Beauchamp, J. Am. Chem. Soc. 106 (1984) 7336.
[52] S.G. Lias, P. Ausloos, J. Am. Chem. Soc. 92 (1970) 1840.
[53] S.G. Lias, P. Ausloos, J. Res. Natl. Bur. Stand. Sec. A: Phys. Chem. 75 (1971) 589.
[54] T. Hsieh, J.P. Gilman, M.J. Weiss, G.G. Meiseis, J. Phys. Chem. 85 (1981) 2722.
[55] R. Feng, C. Wesdemiotis, M. Zhang, M. Marchetti, F.W. McLafferty, J. Am. Chem. Soc. 111 (1989) 1986.
[56] P. Jungwirth, T. Bally, J. Am. Chem. Soc. 115 (1993) 5783.
[57] Z. Qu, X.-D. Zhang, X. Ai, J.-P. Zhang, X.-K. Zhang, Q. Zhang, Chem. Phys. Lett. 360 (2002) 283.
[58] W.J. Van der Hart, J. Am. Soc. Mass Spectrom. 10 (1999) 575.
[59] K.C. Hunter, A.L.L. East, J. Phys. Chem. A 106 (2002) 1346.
[60] K.M. Ervin, S. Gronert, S.E. Barlow, M.K. Gilles, A.G. Harrison, V.M. Bierbaum, C.H. DePuy, W.C. Lineberger, G.B. Ellison, J. Am. Chem. Soc. 112 (1990) 5750.
[61] A.A. Zavitsas, J. Phys. Chem. A 107 (2003) 897.